Advances in Science and Technology Research Journal

Advances in Science and Technology Research Journal 2024, 18(2), 129–142
https://doi.org/10.12913/22998624/184100
ISSN 2299-8624, License CC-BY 4.0

Received: 2024.01.18
Accepted: 2024.02.14
Published: 2024.03.14

Enhancing Electrical Discharge Machining Performance by Mixing Nano Chromium Trioxide Powder with Soybean Dielectric to Machine Inconel 718 Alloy

Dunya Adnan Ghulam[1*], Abbas Fadhil Ibrahim[1]

[1] Production Engineering and Metallurgy Dept., University of Technology-Iraq, Alsina'a street, 10066 Baghdad, Iraq

* Corresponding author's e-mail: dunia.adnan9@yahoo.com

ABSTRACT

Inconel 718 super alloy is suitable for components exposed to high temperatures and demanding high strength; it is one of the hardest alloys to machine by conventional processes due to its properties. Nano Powder mixed electrical discharge machining is one of the most sophisticated processes to produce precise three dimensional complicated forms of hard metals through a thermo-physical process, so it is suitable for machining Inconel 718. This study reports an experimental investigation to improve the machining performance of Inconel 718 super alloy by adding nano chromium oxide powder particles to biodegradable and renewable soybean oil, which is used as a dielectric fluid to preserve the environment, with a magnetic field to assist in improving the process performance. The effects of machining parameters, namely peak current, pulse on time, powder concentration, and magnetic field on the responses in terms of white layer thickness, heat affected zone, surface roughness, material removal rate, and surface crack density were investigated. The observed results manifested that the addition of nano chromium oxide particles to dielectric fluid enhances the process performance. The white layer thickness and heat affected zone improved by 43.93% and 48.82%, respectively. The enhancements in measured surface roughness and material removal rate were 51.76% and 20.62%, respectively. Micrographs of scanning electron microscope verifies that the number of cracks on the machined surface with 4 g/l of nano Cr_2O_3 powder addition was reduced by half, and surface crack density improved by 10.31%, in comparison to machining without powder addition. It is observed that the current had the largest effect on the responses, followed by powder concentration, pulse on time, and magnetic field.

Keywords: NPMEDM, Inconel 718 alloy, Nano Cr_2O_3, surface integrity, magnetic field assistance.

INTRODUCTION

The application of Inconel 718 for components performing in particularly demanding conditions is determined by its properties. It is extensively utilized in combustion chambers, blades, turbine disks, etc. The challenges associated with machining nickel based alloys made it very difficult to machine using conventional processes [1]. Electrical discharge machining (EDM) is widely used to meet the requirements of the current industries, which need to machine super alloys easily while enhancing their mechanical properties [2]. The EDM is an unconventional machining process that is broadly used to machine metals with high toughness that are highly difficult to machine with conventional processes, such as the Inconel 718 alloy. Up to now, EDM is used in many industries to machine molds, dies, aerospace, and many other industries. Its working principle depends on the thermo-electrical process to remove the metal from the machined surface in the presence of dielectric fluid without any touch between the electrode and the machined surface [3]. Some problems in the EDM process are restricting its applications, such as its high surface roughness and its low efficiency of machining. Thus, the powder addition to the dielectric fluid is a proven

technique to overcome these problems; the name of this technique is the powder mixed electrical discharge (PMEDM) process, which provides advantages in terms of economic and quality. The added powders assist in increasing the distance of the spark gap that forms between the machined surface and the electrode tool and also lead to less insulating strength of the dielectric fluid. As a result, the process becomes more stable, improving the material removal rate significantly and reducing the roughness of the machined surface [4].

There are many researchers that have done studies and tried to develop and improve the PMEDM. S. Ramesh et al. studied the machining of Nimonic 75 using graphite, silicon, and manganese powders. As a result, the highest MRR was yielded with graphite powder, and a good surface roughness was produced using silicon powder for the machined specimens [5]. In the context of nano PMEDM, the addition of the nano particles of (Al_2O_3) and (SiO_2) to the deionized water to machine the Ti-6Al-4V alloy was studied. The results manifested that the lowest thickness of the recast layer and the value of cracks for the machined surface were obtained at 75% Al_2O_3-SiO_2 and 25% relative composition [6]. To develop the technique of removing the debris from the machining gap, a magnetic field is used. Using a magnetic field helps generate forces that act on the debris from a distance (i.e., without contact) [7]. Preetkanwal Singh Bains et al. witnessed that the magnetic field has a significant effect on the MRR and Ra, and the micro-hardness and the white layer thickness are reduced due to the effect of it [8]. Micro and nano particle sizes of chromium with the addition of Span-20 into the dielectric were investigated to machine AISI D2 hardened steel in [9] after comparison between micro-nano chromium and the used surfactant. The results evinced that the nano chromium and Span-20 have achieved the best results in productivity. Machining of Inconel 718 using graphene nano fluid was done by [10]. Results elucidated that the machining performance was improved by using grapheme nanofluid. In [11], the conventional EDM was modified by adding nano (Al_2O_3) into deionized water to machine Inconel 825. An improvement in MRR and surface roughness of up to 57% and 63%, respectively, was achieved in comparison with the conventional EDM process.

Inconel 718 super alloy is utilized in many assorted applications, such as different engine parts, die casting of metals, and other important applications, due to its high strength, toughness, and corrosion resistance. Due to the paucity of studies available on the machining of Inconel 718 by adding nanoparticles, in the present study, NPMEDM was used to machine Inconel 718 alloy by adding nano Cr_2O_3 powder to a biodegradable and renewable dielectric (soybean oil SBO) with the incorporation of magnetic field assisted techniques because there haven't been any studies on machining Inconel 718 super alloy using nano Cr_2O_3 powder addition with magnetic field assistance to improve its surface integrity. Practical experiments were carried out after being designed using a general full factorial multi-level design to investigate the impact of current, pulse on the time, powder concentration, and magnetic field on the surface integrity.

MATERIALS AND METHODS

The NPMEDM process was used to machine Inconel 718 super alloy in the present study; the dimensions of the workpieces were 25×10×4 mm. Copper was used as an electrode with dimensions of 15×10×70 mm. Copper has a good melting point of 1083.4 °C, which is the most crucial factor in determining electrode wear rate. It also has a proper thermal conductivity of 398 W/m·K. These thermal properties make copper a good choice as a tool electrode.

Nano Cr_2O_3 powder of 80 nm particle size has been added to soybean oil (SBO), which has been used as a dielectric fluid because it is a biodegradable and renewable oil and also has a little vaporization loss and stable viscosity. Surfactant was needed to maintain the powder particles suspended in the dielectric fluid and prevent them from settling down into the bottom of the machining tank; therefore, Tween 60 was used for this purpose. Two pieces of neodymium magnet (NdFeB) were used as a permanent magnet to generate a magnetic field; its intensity was (0.2 T). A digital gaussmeter model (DGM-102) was utilized to measure the magnetic field intensity. A tank shown in Figure 1 made of galvanized iron with dimensions of 500×200×250 mm was fabricated to be employed as a machining tank. It was tooled up with a circulation system that consisted of a pump, a flushing nozzle, and a 5 mm diameter pipe. This pipe was fastened around the inside walls of the machining tank. The pipe has eight holes, each with a diameter of one millimeter, and was distributed in an

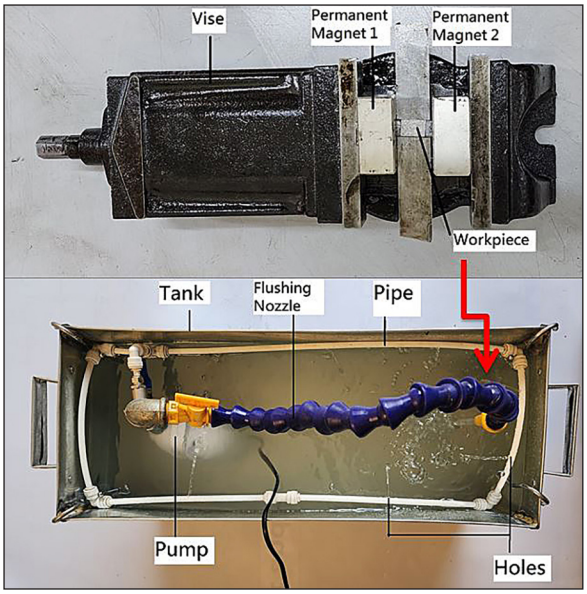

Figure 1. Machining tank

even manner throughout the pipe length. This pipe helps with the delivery and recirculating of the dielectric fluid that contains the powder particles in the machining tank, which prevents the powder particles from settling down in the machining tank during the machining process.

Experimental procedure

During the magnetic field-assisted NPMEDM process, voltage is applied to both the workpiece and electrode tool, which leads to the generation of an electric field in the machining gap, which contains nano Cr_2O_3 particles. These particles get energized and move in free motion due to Lorentz forces that originate from the use of a permanent magnet, which contribute to transforming the free movement into organized movement, which leads to the improved performance of NPMEDM process. Dielectric fluid was flushed into the machining gap through the flushing nozzle; the scheme of the process is shown in Figure 2. The flow chart of the experiment depicted in Figure 4.

The practical experiments were designed and analyzed using multi-level general full factorial design by Minitab software. 24 experiments were conducted using four input parameters. Constant and varied parameters with their levels that were used during the machining process are listed in Tables 1 and 2, respectively. A snapshot of the machined specimen using these parameters is depicted in Figure 3. After conducting the experiments, WLT, HAZ, SCD, Ra, and MRR were computed as responses.

Measurement of experimental responses

The thickness of heat-affected zone containing a hardened layer and a recast layer (the white layer), was measured using an optical microscope. The samples were prepared suitably before measuring the thickness of the white layer (Figure 5). The samples were mounted using a suitable mold to facilitate the grinding using emery paper of grit size (100, 500, 1000, 1200, 2000) and polishing processes using alumina powder with polishing paper, then the etching process was conducted using an etch solution consisting of HCl, HNO_3, H_2O, and glycerin. After the etching process, the samples were washed with water and alcohol and

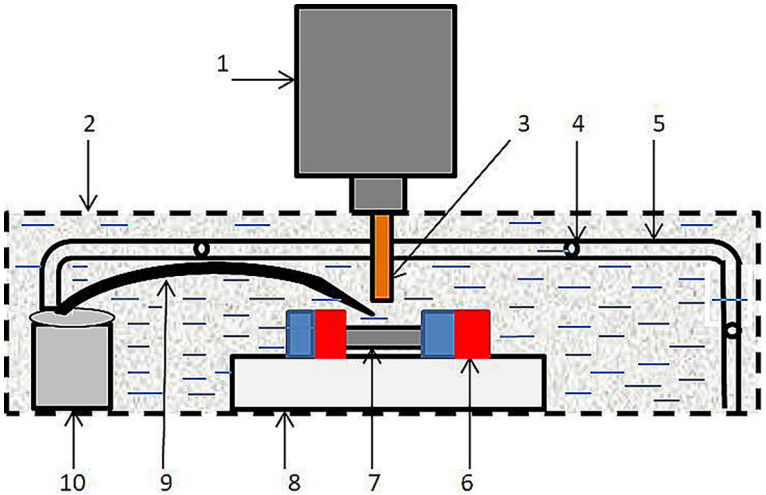

Figure 2. Scheme of MF-NPMEDM: (1) Servo system, (2) machining tank, 3) electrode, (4) hole, (5) pipe, (6) pair of permanent magnets, (7) workpiece, (8) vise, (9) flushing nozzle, (10) pump

Figure 3. Specimen before and after machining

then dried. The average thickness of the white layer and heat affected zone was measured at 400× magnification using an optical microscope type OPTICA, MET Series, Italy.

Three measurements using the Maher Fedral Pocket Surf PS1 surface roughness tester were made for each of the 24 machined workpieces in order to determine the specimen's surface roughness. The average of the three measurements was then calculated.

MRR is the difference in weight of the specimen before and after machining divided by machining time, it was calculated using Equation 1.

$$MRR = (W_b - W_a) / \rho \cdot t \text{ mm}^3/\text{min} \quad (1)$$

where: W_b – the weight of the workpiece before machining (g), W_a – weight of the workpiece after machining (g), ρ – Inconel 718 density (0.00822 g/mm^3), t – machining time (min).

Surface crack density (SCD) was measured in terms of the number of microcracks and their length. To determine the SCD of the machined surface; the measured average length of micro cracks was divided by the area of the micrograph, which was captured using an Axia ChemiSEM-Thermo Scientific device to get the SCD through Equation 2.

$$SCD = CL/A \text{ μm}/\text{μm}^2 \quad (2)$$

where: CL – average crack length (μm), A – micrograph area (μm^2).

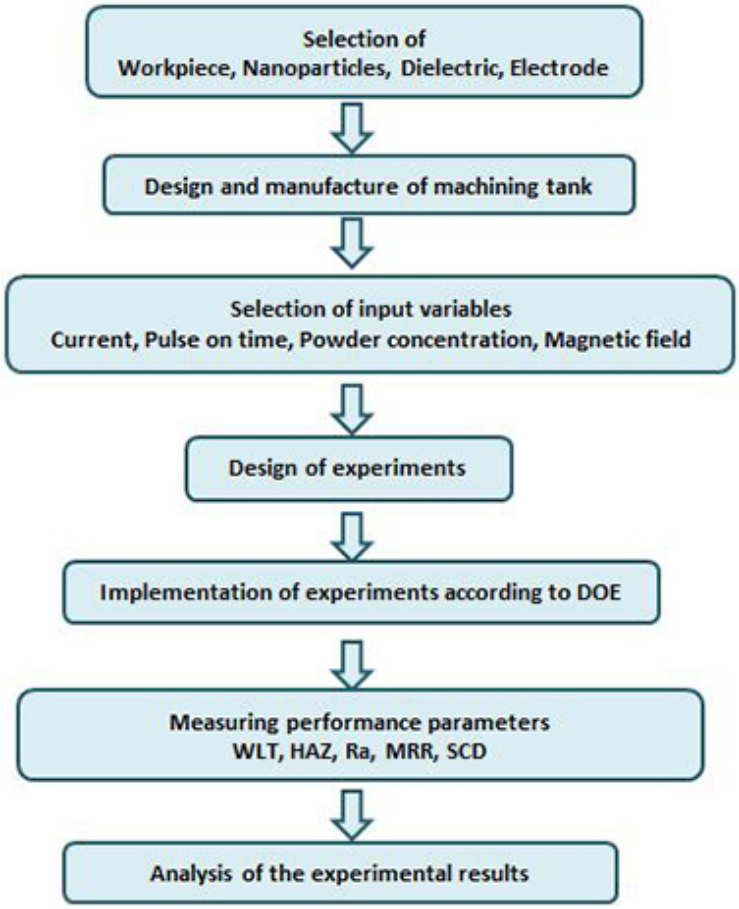

Figure 4. Flow chart of experiment

Table 1. Constant parameters

Parameters		Unit	Value
Electrical parameters	Pulse off time	(μs)	75
	Polarity	/	Straight
	Gap voltage	(V)	240
Non-electrical parameters	Dielectric fluid	/	Soybean oil
	Electrode type	/	Copper
	Powder type	/	Cr_2O_3
	Particles size	nm	80
	Surfactant type	/	Tween 60
	Surfactant concentration	(ml/l)	1
	Depth of cut	(mm)	1

Table 2. Levels of variable parameters

Parameters	Units	First level	Second level	Third level
Current	(A)	8	16	/
Pulse on time	(μs)	100	200	/
Concentration	(g/l)	0	2	4
Magnetic field	(T)	0	0.2	/

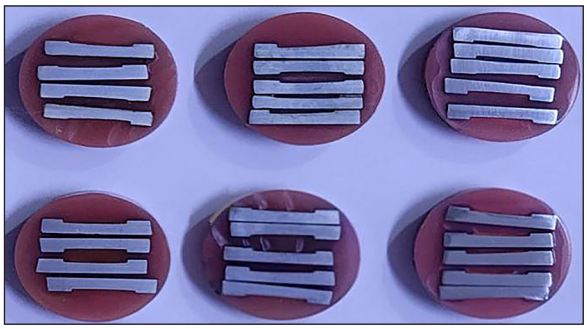

Figure 5. Prepared samples for measuring white layer thickness

RESULTS AND DISCUSSION

Parameters affecting the white layer thickness

During the NPMEDM process, the surface layer changes due to the occurrence of thermal processes, which cause changes in the microstructure of the machined surface and lead to defects such as micro cracks. Heat-affected zone consists of a white layer (recast layer) and a hardened layer as mentioned, and the white layer thickness of the machined surface is an important factor that affects the surface quality; therefore, it is measured to examine the surface quality [12]. In the PMEDM process, uniform plasma energy is obtained due to the better electrical and thermal properties of the added powder to the dielectric. This insulating medium produces a white layer with the least thickness and regular distribution over the machined surface as compared with the traditional EDM process [13]. The machined surface is melted, and debris is formed during the pulse on time due to the elevation of the temperature to very high levels in the machining zone. The melted debris accumulates and is re-solidified in the machining zone during the pulse off time while the discharging process takes place, thus the white layer is formed as a result of the re-solidification of the melted debris in the machining zone. Insufficient flushing of debris by the insulating fluid causes sedimentation of it, which leads to an increase in the thickness of white layer. After the addition of nano Cr_2O_3 particles to the insulating fluid, the white layer thickness decreased because of the presence of these particles in the machining gap; the distance between the workpiece and electrode tool became larger, which led to a better flushing method; also, a wider plasma channel could be obtained, so a wider machined distance is covered with a more uniform energy distribution, thus the white layer thickness was decreased. On the other hand, the use of a special circulation system to circulate the insulating fluid improved the efficiency of the flushing mode, which also contributed to obtaining a thinner white layer.

Applied current with a higher value causes deposition and more migration to the molten material, so a thicker layer is obtained. Similar to the current effect, an increment in pulse on time causes the white layer thickness to increase because of the higher discharge energy in the plasma

channel, and the insulating fluid becomes not capable to evacuate the debris from the machining gap; therefore, the debris reattaches and solidifies on the machined surface, hence the thicker white layer produced; therefore, applying current and pulse on time with lower values produces a thinner white layer. Magnetic field causes a slight increase in the thickness of the white layer. Increasing the concentration of nano Cr_2O_3 from (2) g/l to (4) g/l leads to an increase in the white layer thickness. When the concentration of the added powder increases, a short circuit or arcing will happen, causing the NPMEDM process to become unstable and the melted material to precipitate and a thicker white layer to be produced. The effects of these parameters on the white layer thickness are evinced in Figure 6.

The experimental results of the experiments, which have been designed with a general full factorial design, are displayed in Table 3. As a result, the thinnest white layer and the heat-affected zone that were obtained (26.36) µm and (52.737) µm, respectively, at the lower value of the used concentration (2) g/l of nano Cr_2O_3 and at the current applied with (16) A, the value of pulse on time was (100) µs and without the use of a magnetic field. On the other hand, it was observed that the thickest white layer was obtained with an amount of (54.54) µm; it was produced when using a concentration of (4) g/l of Cr_2O_3, applying a discharge current of (16) A, a pulse on time of (200) µs, and using a value of magnetic field with an intensity of (0.2) T. When applying the values of discharge current with (8) A, pulse on time (200) µs, Cr_2O_3 with a concentration of (2) g/l, and magnetic field intensity value with (0.2) T, it was noticed that the thickest heat-affected zone was obtained with an amount of (143.64) µm. An optical microscope was used to measure the white layer and the heat affected-zone thickness. The obtained microscopic images are illustrated in Figure 7.

The influences of the working parameters were analyzed by Minitab software. The analysis of variance, which represents the most significant parameters on the average white layer thickness, is manifested in Table 4. The models are statistically significant according to the P-values, which are less than 0.05, which means the confidence level is 95%. It was noticed that the current was the most effective parameters, followed by concentration and pulse on time. Magnetic field has the lowest effect on the white layer thickness. X-ray diffraction (XRD) test was made for samples that were machined with and without the addition of 4 g/l of nano Cr_2O_3, as shown in Figures 8a and 8b respectively. This results in a γ phase of (111) at (43.45°), (200) at (50.78°), and (220) at (74.67°). While the phase of (Cr_2O_3) that was deposited on the surface of Inconel 718 appeared in one very small peak, which is (300) at (65.31°) angle, The spectrum is consistent with a solid solution of austenite, with a face axis cube (fcc) of Ni-Cr (a = 0.359 nm in the Fm-3m group) and the dominant matrix being displayed. In order to confirm the presence of the chromium (III) oxide phase, X-ray diffraction (XRD) measurements were conducted. The rhombic structure was identified with the help of Multimodal JCPDS Card 74-0326 of the Cr2O3 structure. The peaks observed are attributed to the a-Cr2O3 phase, with unit cell parameters of a = 4.96070 and c = 13.59900 (˚A).

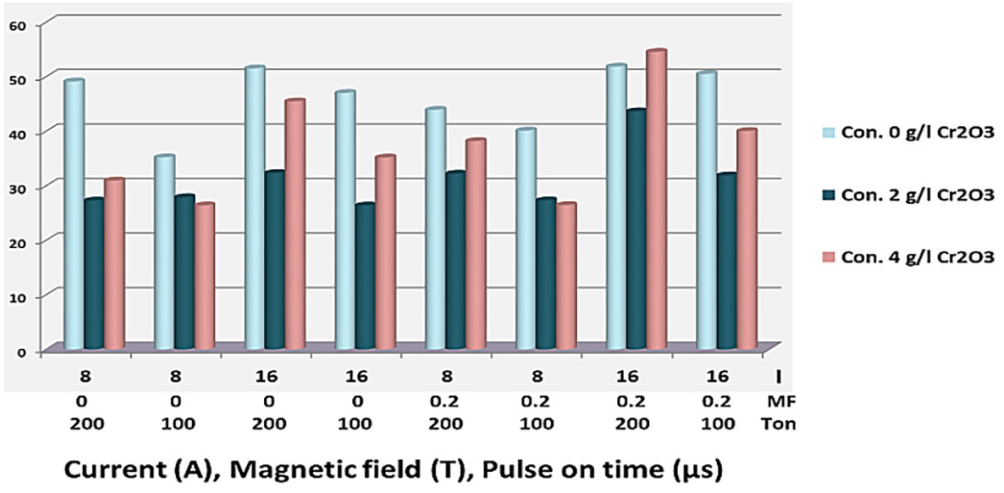

Figure 6. Effect of current, magnetic field, pulse on time, and concentration on the white layer thickness

Table 3. Provides experimental results for the average WLT, HAZ and Ra and MRR

Run	Current (A)	Ton (µs)	Con (g/l)	MF(T)	Average WLT (µm)	Average HAZ (µm)	Average Ra (µm)	MRR (mm^3/min)
1	16	200	0	0.2	51.845	115.21	5.297	9.033
2	8	200	2	0.2	32.187	143.64	3.681	3.548
3	16	100	4	0.2	40.007	123.627	5.548	10.829
4	8	100	4	0	26.385	96.36	3.901	3.655
5	8	200	4	0	30.933	98.176	3.958	3.875
6	8	200	0	0	49.12	93.34	4.457	3.766
7	8	100	0	0	35.2	94.55	4.879	3.018
8	16	100	0	0.2	50.5	73.33	4.828	8.839
9	16	100	2	0.2	31.87	93.635	4.786	10.708
10	8	100	4	0.2	26.435	110.91	4.293	3.367
11	8	200	0	0.2	43.925	137.495	4.754	3.282
12	16	200	4	0	45.45	130.915	5.143	13.283
13	8	200	2	0	27.27	99.387	3.819	3.789
14	8	100	2	0	27.873	133.63	3.801	3.153
15	16	200	0	0	51.51	111.815	4.737	11.039
16	16	200	2	0.2	43.635	127.263	5.742	12.519
17	16	100	2	0	26.36	52.737	4.550	9.534
18	8	200	4	0.2	38.18	158.22	4.902	3.565
19	8	100	0	0.2	40.1	92.49	4.569	3.030
20	16	200	4	0.2	54.54	129.113	5.806	12.697
21	16	200	2	0	32.315	62.417	4.245	12.704
22	8	100	2	0.2	27.3	102.72	2.204	3.275
23	16	100	4	0	35.167	98.175	4.791	9.764
24	16	100	0	0	47.017	103.023	4.304	10.401

Parameters affecting the surface roughness

In the NPMEDM, the discharge gap expanded as a consequence of the nanoparticles distributing the discharge throughout the machined surface. Furthermore, the presence of these nanoparticles causes a lower discharge energy, which in turn makes it possible to deliver heat in a localized way with higher precision and proper control, resulting in better surface finish [14].

The measured Ra in this study achieved lower values than those of [15], in which Inconel 718 was machined without powder addition. The observed Ra values varied from 3.8 µm to 8.7 µm when the current was increased from 3 A to 9 A, while after adding nano Cr_2O_3 in this study, the measured Ra varied from 2.204 µm to 5.806 µm when the current was increased from 8 A to 16 A due to the positive effect of nano Cr_2O_3.

Furthermore, powder addition to the dielectric makes the flushing mode more efficient by enlarging the machining gap, thereby obtaining better surface finish. Moreover, the experimental results elucidated that adding nano Cr_2O_3 with a concentration of 2 g/l gave better results compared to a 4 g/l concentration of added nano Cr_2O_3. More electrical discharge density happened when a 4 g/l concentration was used, hence a deeper crater produced and finally a rougher surface. As well, at a high powder concentration, more powder

Table 4. Analysis of variance for the white layer thickness

Source	DF	Adj SS	Adj MS	F-Value	P-Value
Model	7	1853.20	264.74	22.06	0.000
Linear	5	1781.06	356.21	29.68	0.000
Current	1	462.06	462.06	38.50	0.000
Ton	1	313.18	313.18	26.10	0.000
Con.	2	917.94	458.97	38.24	0.000
MF	1	87.87	87.87	7.32	0.016
2-Way interactions	2	72.14	36.07	3.01	0.078
Current·Con	2	72.14	36.07	3.01	0.078
Error	16	192.02	12.00		
Total	23	2045.22			

particles precipitate on the machined surface, and arcing for electrical discharge (discharge instability) will occur, hence the rougher surface finish obtained. At every EDMed surface, discharge spots are generated by electrical discharge; that way, craters are produced, whose size depends on the applied discharge energy. Spark intensity increases with increasing applied current; thus, larger and deeper craters are formed, which attend more damage to the surface finish. Consequently, an increase in the applied discharge current value 8 A to 16 A has a negative effect on the quality of the machined surface and leads to a rougher surface. It was also noticed that increasing the applied pulse on time value of 100 µs to 200 µs resulted in higher surface roughness. The combined influence of parameters on the surface roughness is displayed in Figure 9. Moreover, magnetic

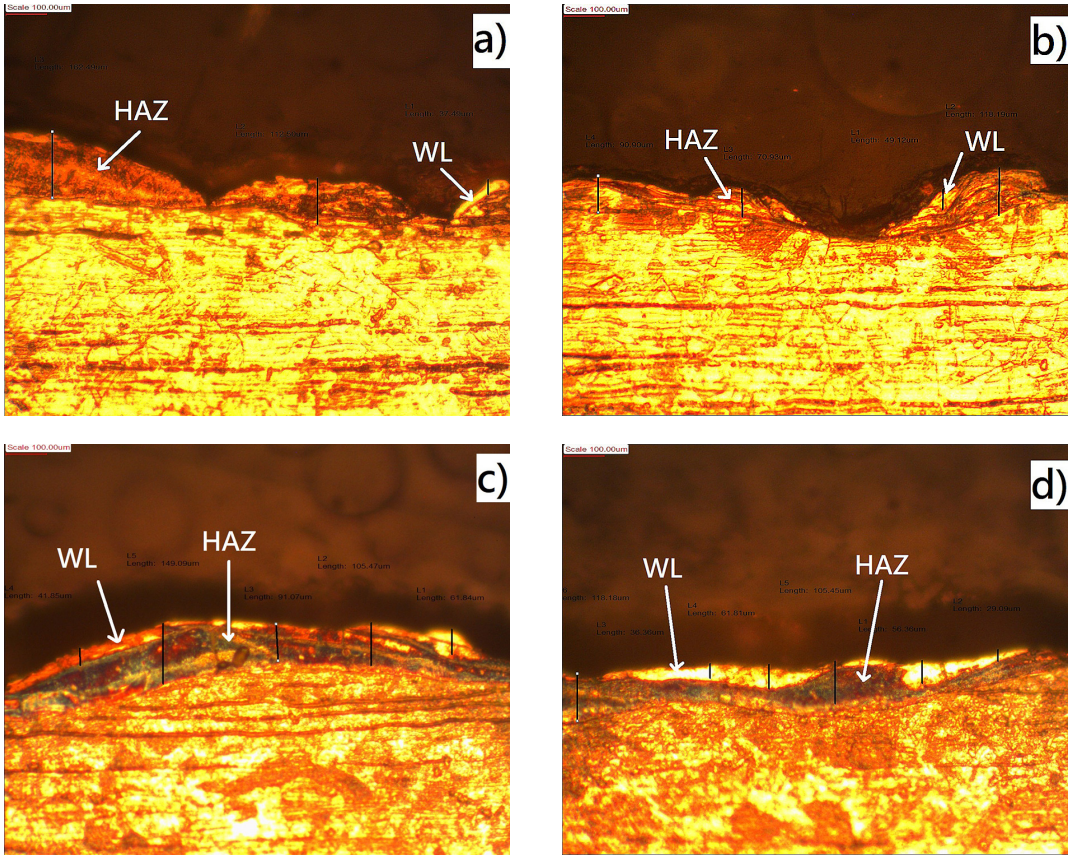

Figure 7. Optical microscopic pictures for the machined specimens:
(a) I(8) A, Ton (200) µs, Con(0) g/l, MF(0.2) T; (b) I(8) A, Ton (200) µs, Con(0) g/l, MF(0) T;
(c) I(16) A, Ton (200) µs, Con(0) g/l, MF(0.2) T; (d) I(16) A, Ton (200) µs, Con(0) g/l, MF(0) T

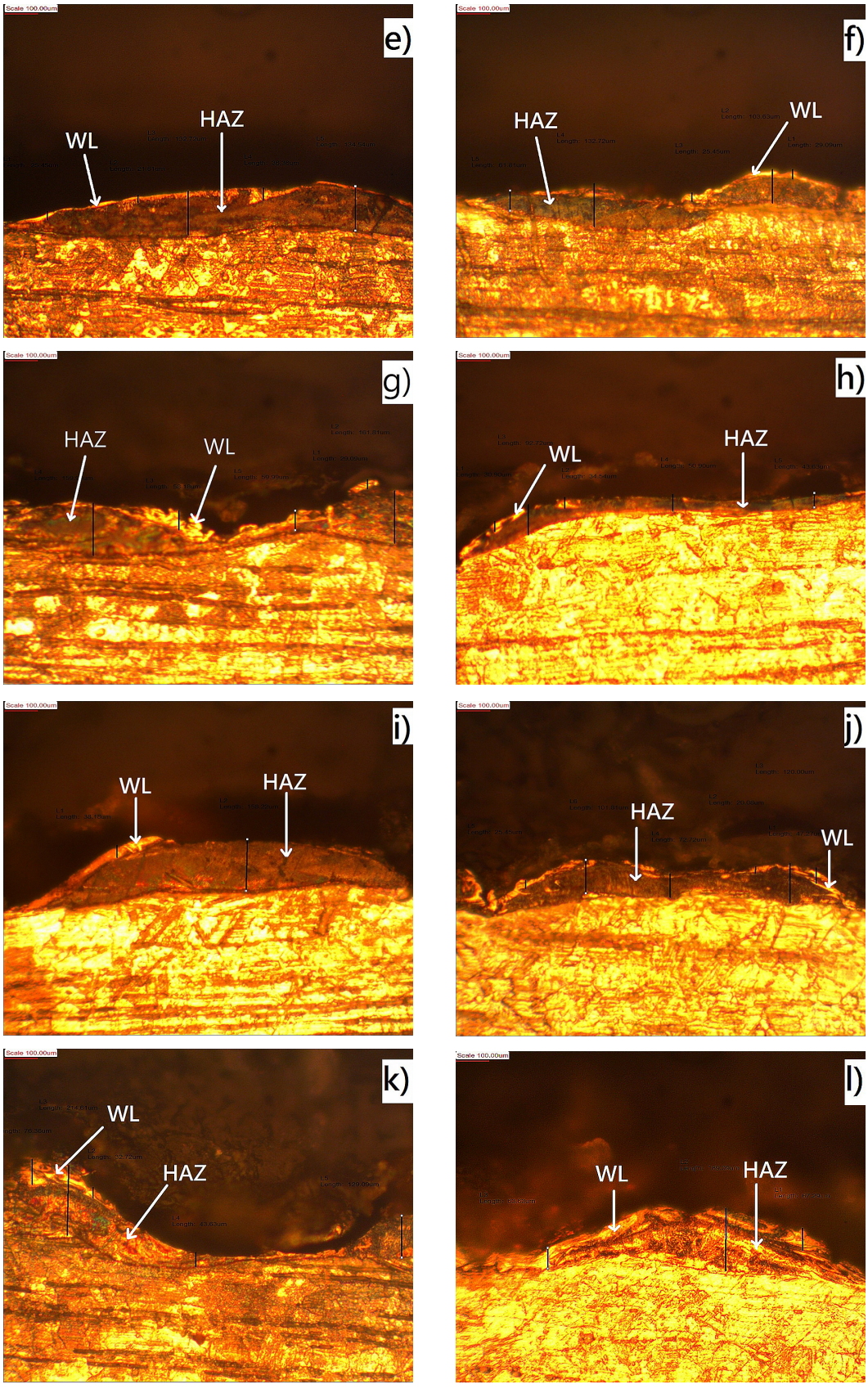

Figure 7. Optical microscopic pictures for the machined specimens:
(e) I(8) A, Ton (200) µs, Con(2) g/l, MF(0.2) T; (f) I(8) A, Ton (200) µs, Con(2) g/l, MF(0) T;
(g) I(16) A, Ton (200) µs, Con(2) g/l, MF(0.2) T; (h) I(16) A, Ton (200) µs, Con(2) g/l, MF(0) T;
(i) I(8) A, Ton (200) µs, Con(4) g/l, MF(0.2) T; (j) I(8) A, Ton (200) µs, Con(4) g/l, MF(0) T;
(k) I(16) A, Ton (200) µs, Con(4) g/l, MF(0.2) T; (l) I(16) A, Ton (200) µs, Con(4) g/l, MF(0) T

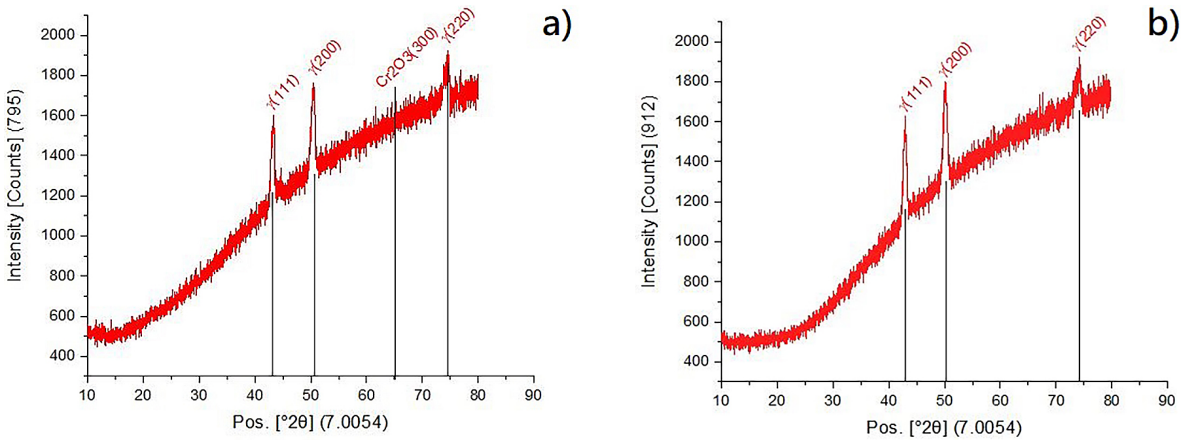

Figure 8. XRD for samples machined at I 16 A, Ton 200 µs, MF 0.2T, with (a) 4 g/l of nano Cr_2O_3 addition, (b) without adding nano Cr_2O_3

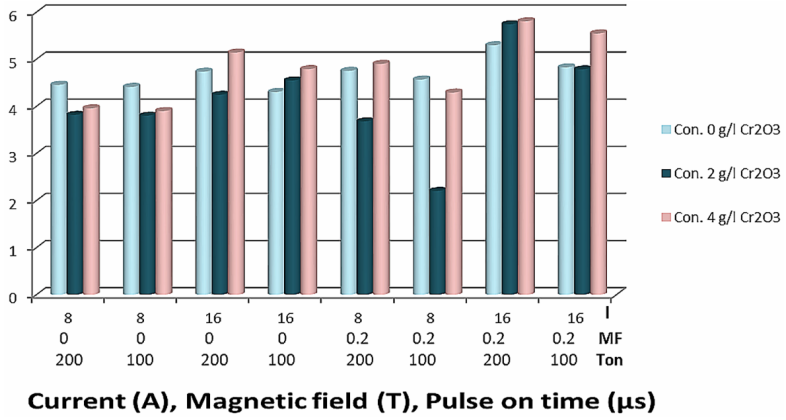

Figure 9. Effect of applied parameters on the surface roughness

field has a little effect on the surface roughness and show a lower surface finish. The minimum surface roughness obtained was 2.204 µm when the parameters with the values of 8 A current, 100 µs pulse on time, 2 g/l powder concentration, and 0.2 T magnetic field intensity were applied, as portrayed in Table 3. The rougher measured surface was at the highest applied machining parameters, i.e., at current of 16 A, pulse on time of 200 µm, Cr_2O_3 of 4 g/l, and using a magnetic field with an intensity of 0.2 T, and it was 5.806 µm. Furthermore, it can be noticed that when applying a magnetic field with a low applied current, it has a positive effect on surface roughness, as in experiments 2 and 22, in which the best roughness was obtained; conversely, when applying a magnetic field with a high applied current 16 A, it has a negative effect and leads to an increase in surface roughness, as demonstrated by experiments 9 and 16 within Table 3. The analysis of experimental results for surface roughness and parameter relationships manifested that the current had the largest effect on the surface finish, followed by powder concentration, pulse on time, and magnetic field. It is noticeable that the model of the analysis of variance for surface roughness is statistically significant, as shown in Table 5.

Parameters affecting the material removal rate

Material removal rate is an important indicator of NPMEDM process performance. This is because it is a determining factor for the machining time of the process, and from an industry perspective, it is a benchmark for the machining process. Adding powder to the insulating fluid reduces its breakdown strength, and powder particles serve to enhance the bridging in the machining gap, which improves the material removal rate of the machined surface [16].The existence of Cr_2O_3 particles in soybean dielectric increases

Table 5. Analysis of variance for the surface roughness

Source	DF	Adj SS	Adj MS	F-Value	P-Value
Model	9	11.6333	1.2926	8.53	0.000
Linear	5	8.2660	1.6532	10.91	0.000
Current (A)	1	4.6441	4.6441	30.66	0.000
Ton (µs)	1	0.6950	0.6950	4.59	0.050
Con. g/l	2	2.3172	1.1586	7.65	0.006
MF (T)	1	0.6097	0.6097	4.03	0.065
2-Way Interactions	4	3.3674	0.8418	5.56	0.007
Current·Con	2	1.8582	0.9291	6.13	0.012
Current·MF	1	0.9009	0.9009	5.95	0.029
Ton·MF	1	0.6082	0.6082	4.02	0.065
Error	14	2.1207	0.1515		
Total	23	13.7540			

the number of sparks in the machining gap during pulse on time, reducing the required time to breakdown the dielectric. Besides, Cr_2O_3 acts as a good transformer of ions to the machined surface. As powder concentration is a vital parameter, it shows that an increment in powder concentration leads to an increase in MRR as compared to the experiments conducted without powder addition.

The positive effects of current lead to enhanced MRR, where when the current increases, the energy of the sparks increases too. Also, a higher impulse force is generated in the machining gap, which heats the machined surface, resulting in more melting and evaporation for the machined surface, i.e., an increase in MRR. Comparable to the current effect, an increment in pulse on time causes an increase in MRR because the machined surface is exposed to a strong heat effect as a result of converting the discharge energy to high thermal energy, which melts and vaporizes the workpiece surface. Increasing the nanoparticle Cr_2O_3 concentration to 4 g/l produced the greatest MRR, which was 13.283 mm^3/min. When the applied current was 16 A, the pulse on time was (200 µs). Without using a magnetic field (Table 3). Applying current with a value of 16 A improved the MRR largely as compared to applying current with a value of 8 A, as shown in Figure 10.

Parameters affecting the surface crack density

Typically, EDMed surface features, including globules of debris, pockmarks, overlapping craters, and cracks, which indicate subpar surface quality, have been the main issues with EDM over the years. Among others, cracking is an extremely significant surface imperfection [17]. The difference in temperature between the

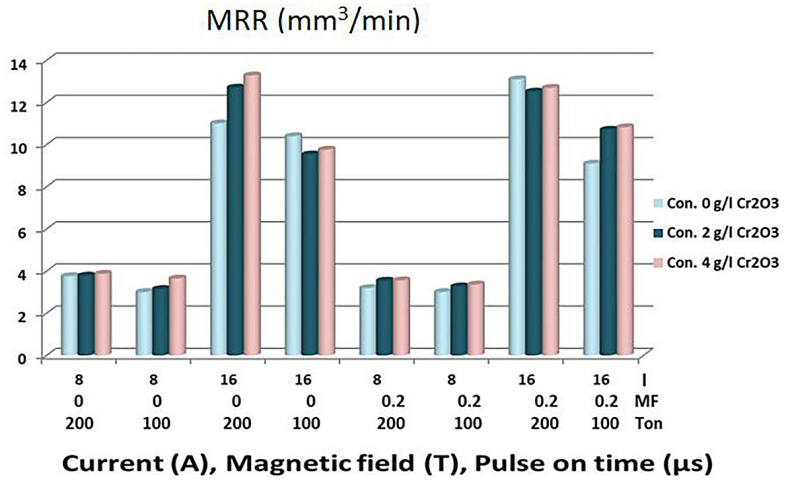

Figure 10. Effect of applied parameters on the material removal rate

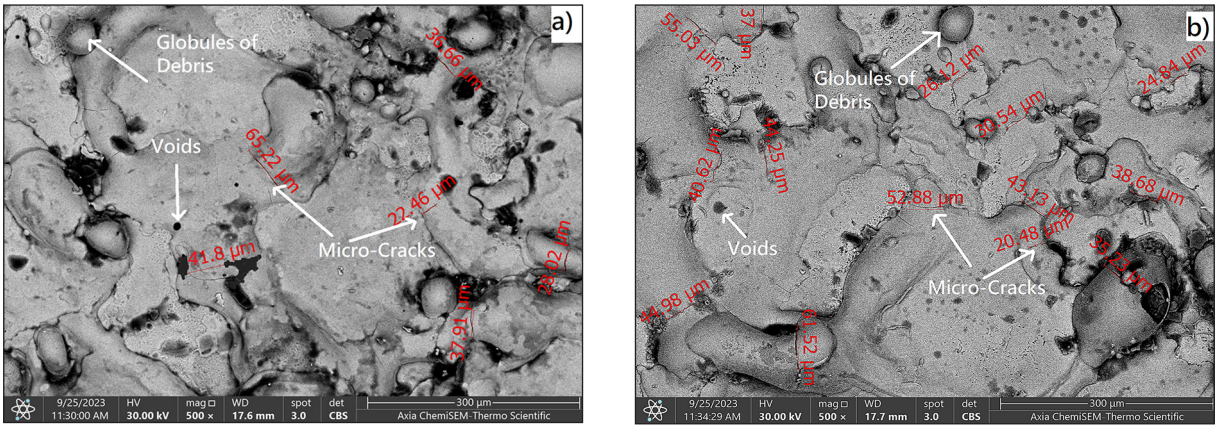

Figure 11. Cracks of the machined surface at 500X magnification, I 16 A, Ton 200 µs, MF 0.2T, with (a) 4 g/l of nano Cr_2O_3 addition, (b) without adding nano Cr_2O_3

machined surface and the surrounding area generates a rapid cooling rate, which causes the yield stress to rise quickly. Rapid solidification hinders the molten metal from contracting, developing tension parallel to the surface of the machined workpiece and creating cracks within the surface. A component may fail as a consequence of these cracks because they reduce its fatigue and corrosion resistance [18]. Elevated temperature is generated near the machined surface because of the sparks. The top surface cools faster than the subsurface, therefore higher shrinkage occurs in the subsurface than the top surface; this difference leads to thermal stress development within the machined material (Inconel 718). When these thermal stresses override the ultimate tensile strength of the Inconel 718 material, the micro cracks are produced [19].

Micro cracks developed at higher pulse on time and peak current values due to an increase in discharge energy [20]. The increment in impulsive forces and discharge energy, which is a function of current and pulse on time, results in the removal of more material, thereby generating larger craters. Increasing the pulse on time affects the texture of the machined surface, which consists of the different sizes of deep craters and overlapping rims that were created because of sequential electrical discharges, extreme temperatures, and the melting or vaporization of the machined material. As a result, the thermal tendency within the solidified layer increases, therefore greater residual stresses being generated and an increase in the SCD. Using magnetic field assistance helps in removing the debris from the machining gap effectively, which will reduce the occurrence of abnormal discharge and lessen the length of the cracks. In order to eliminate the surface defects and micro cracks addition of powders to the dielectric technique was used. Adding the powder to the dielectric leads to increasing the frequency of the sparks and reducing the discharge energy with a larger number of sparks in the machining zone. Furthermore, the existence of powder particles in the dielectric fluid causes the plasma channel to enlarge and become wider; thereby, the thermal energy transferred to the machined surface is uniformly distributed among the larger areas. The cracks were reduced with regard to the reasons mentioned above, which led to a decrease in thermal stresses and the solidification of the shrinkages.

The findings revealed that the most significant factors impacting the surface properties were the highest applied level of current of 16 A, pulse on time of 200 µm, and using a magnetic field with an intensity of 0.2 T; therefore, these factors were selected for the SEM examination. Throughout the SEM micrographs, it was revealed that the machined surface has complex appearances, like voids, globules of debris, and cracks, which are considered disappointing morphologies, as elucidated in Figures 11 a and 11 b. The SCD of the surface machined by NPMEDM has a smaller number of cracks as compared with the surface machined without the addition of nano Cr_2O_3. The SCD of this study was calculated in terms of average crack length (µm) divided by micrograph area (µm^2), the SCD for machined surface with the added 4 g/l of nano Cr_2O_3 powder and fixing other process parameters was 0.00322 µm/µm^2, and the SCD for machined surface without powder addition was 0.00359 µm/µm^2.

CONCLUSIONS

In the present study, the NPMEDM process was used to machine the Inconel 718 super alloy, process performance in terms of WLT, HAZ, Ra, MRR, and SCD was studied. Nano Cr_2O_3 powder was added to soybean oil, which was used as an insulating fluid. The effects of process parameters, such as current, pulse on time, powder concentration, and magnetic field were investigated and analyzed by Minitab using a general full factorial multi-level design. The following conclusions were drawn:

- experimental results manifested that adding nano Cr_2O_3 powder to dielectric fluid improved the performance of the process in terms of all responses,
- increasing the current value from 8 A to 16 A led to improved WLT, HAZ, and MRR but a rougher surface was obtained;
- increasing the pulse on time from 100 µs to 200 µs has a negative effect on the WLT, HAZ, and Ra but improved the MRR;
- magnetic field with an intensity of 0.2 T has no effect on the WLT, HAZ and MRR but improves the Ra;
- the current had the largest effect on the responses, followed by powder concentration, pulse on time, and magnetic field;
- the thinnest white layer and the heat-affected zone that being obtained were 26.36 µm and 52.737 µm, respectively. They were obtained at the lower value of the used concentration 2 g/l of nano Cr_2O_3 and at the current applied with 16 A, at pulse on time with a value of 100 µs, and without the use of a magnetic field;
- the minimum surface roughness obtained was 2.204 µm when the parameters with values of 8 A current, 100 µs pulse on time, 2 g/l powder concentration, and 0.2 T magnetic field intensity were applied;
- increasing Cr_2O_3 nanoparticles concentration to 4 g/l produced greatest MRR; which was 13.2834 mm^3/min, when the applied current was 16 A, pulse on time was 200 µs and without using magnetic field.

NPMEDM is a very important process in machining superalloys, and this study aims to enhance it by obtaining the best properties for the machined surface, but its mechanisms are still insufficiently understood. The endeavors of future studies may investigate the fundamental mechanism more thoroughly. Further studies are needed to fully comprehend how nanoparticle type, shape, and size affect the surface integrity, fatigue, and corrosion resistance of the machined part.

REFERENCES

1. Jarosław B. surface topography of inconel 718 alloy in finishing WEDM. Adv. Sci. Technol. Res. J. 2022; 16(1): 47–61. doi: 10.12913/22998624/142962.
2. Perumal A., Azhagurajan A., Prithivirajan R., Kumar S.S. Experimental investigation and optimization of process parameters in Ti – (6242) alpha–beta alloy using electrical discharge machining. J. Inorg. Organomet. Polym. Mater. 2021; 31(4): 1787–1800. doi: 10.1007/s10904-020-01786-1.
3. Al-Amin M. Assessment of PM-EDM cycle factors influence on machining responses and surface properties of biomaterials: A comprehensive review. Precis. Eng. 2020 Sept; 66: 531–549. doi: 10.1016/j.precisioneng.2020.09.002.
4. Mohanty S., Mishra A., Nanda B. K.,. Routara B. C. Multi-objective parametric optimization of nano powder mixed electrical discharge machining of AlSiCp using response surface methodology and particle swarm optimization. Alexandria Eng. J. 2018 Jun; 57(2): 609–619. doi: 10.1016/j.aej.2017.02.006.
5. Ramesh S., Jenarthanan M. P. Optimizing the powder mixed EDM process of nickel based super alloy. Proc. Inst. Mech. Eng. Part E J. Process Mech. Eng. 2021 Aug; 235(4): 1092–1103. doi: 10.1177/09544089211002782.
6. Oskueyan S., Abedini V.,. Hajialimohamadi A. Effects of hybrid Al2O3- SiO2 nanoparticles in deionized water on the removal rate and surface roughness during electrical discharge machining of Ti-6Al-4V. Proc. Inst. Mech. Eng. Part E J. Process Mech. Eng. 2021. doi: 10.1177/09544089211059311.
7. Zhang Z., Zhang Y., Ming W., Zhang Y., Cao C., Zhang G. A review on magnetic field assisted electrical discharge machining. J. Manuf. Process. 2020 Dec; 64, 694–722. doi: 10.1016/j.jmapro.2021.01.054.
8. Bains P.S., Singh S., Payal S.H. S., Kaur S. Magnetic field influence on surface modifications in powder mixed. Silicon. 2018. doi: 10.1007/s12633-018-9907-z.
9. Nor Ain Jamil Hosni M. A. L. Experimental investigation and economic analysis of surfactant (Span-20) in powder mixed electrical discharge machining (PMEDM) of AISI D2 hardened steel. Mach. Sci. Technol. 2020; 24(2): 1–27. doi: 10.1080/10910344.2019.1698609

10. Paswan K., Pramanik A., Chattopadhyaya S. Machining performance of Inconel 718 using graphene nanofluid in EDM. Mater. Manuf. Process. 2020 Jan; 35(1): 33–42. doi: 10.1080/10426914.2020.1711924.
11. Kumar A., Mandal A., Dixit A. R., Das A. K., Kumar S., Ranjan R. Comparison in the performance of EDM and NPMEDM using Al_2O_3 nanopowder as an impurity in DI water dielectric. Int. J. Adv. Manuf. Technol. 2019; 100(5–8): 1327–1339. doi: 10.1007/s00170-018-3126-z.
12. Machno M., Trajer M., Bizoń W., Czeszkiewicz A. A study on accuracy of micro-holes drilled in Ti-6Al-4V alloy by using electrical discharge machining process. Adv. Sci. Technol. Res. J., 2022; 16(6): 55–72. doi: 10.12913/22998624/155224.
13. Muthuramalingam T. Experimental investigation of white layer formation on machining silicon steel in PMEDM process. Silicon. 2020; doi: 10.1007/s12633-020-00740-7.
14. Paswan K. An analysis of microstructural morphology, surface topography, surface integrity, recast layer, and machining performance of graphene nanosheets on Inconel 718 superalloy: Investigating the impact on EDM characteristics, surface characterizations, and opt. J. Mater. Res. Technol. 2023 Aug, 27: 7138–7158. doi: 10.1016/j.jmrt.2023.11.080.
15. Jafarian F. Electro discharge machining of Inconel 718 alloy and process optimization. Mater. Manuf. Process. 2020; 35(1): 95–103. doi: 10.1080/10426914.2020.1711919.
16. Chaudhari R., Vora J., de Lacalle L. N. L., Khanna S., Patel V. K., Ayesta I. Parametric optimization and effect of nano-graphene mixed dielectric fluid on performance of wire electrical discharge machining process of Ni55.8Ti shape memory alloy. Materials (Basel)., 2021; 14(10): doi: 10.3390/ma14102533.
17. Talla G., Gangopadhyay S., Biswas C. K. Influence of powder-mixed EDM on surface morphology and metallurgical alterations of Inconel 625. Aust. J. Mech. Eng. 2023; 21(5): 1533–1546. doi: 10.1080/14484846.2021.2022580.
18. Paswan K. An Analysis of Machining Response Parameters, Crystalline Structures, and Surface Topography During EDM of Die-Steel Using EDM Oil and Liquid-Based Viscous Dielectrics: A Comparative Analysis of Machining Performance. Arab. J. Sci. Eng. 2023; 48(9): 11941–11957. doi: 10.1007/s13369-023-07626-x.
19. Jadam T., Sahu S. K., Datta S., Masanta M. Powder-mixed electro-discharge machining performance of Inconel 718: effect of concentration of multi-walled carbon nanotube added to the dielectric media. Sādhanā, 2020; 0123456789. doi: 10.1007/s12046-020-01378-2.
20. Srivastava S., Vishnoi M., Gangadhar M. T., Kukshal V. An insight on Powder Mixed Electric Discharge Machining: A state of the art review. Proc. Inst. Mech. Eng. Part B J. Eng. Manuf. 2023; 237(5): 657–690. doi: 10.1177/09544054221111896